



# The Global Regulator MftR Controls Virulence and Siderophore Production in Burkholderia thailandensis

Sudarshan S. Thapa, a\* Ahmed Al-Tohamy, a,b DAnne Grove

Department of Biological Sciences, Louisiana State University, Baton Rouge, Louisiana, USA Cell Biology Department, Biotechnology Research Institute, National Research Centre, Dokki, Cairo, Egypt

ABSTRACT Burkholderia thailandensis is a member of the Burkholderia pseudomallei complex. It encodes the transcription factor MftR, which is conserved among the more pathogenic Burkholderia spp. and previously shown to be a global regulator of gene expression. We report here that a B. thailandensis strain in which the mftR gene is disrupted is more virulent in both Caenorhabditis elegans and onion. The DmftR strain exhib-its a number of phenotypes associated with virulence. It is more proficient at forming biofilm, and the arcDABC gene cluster, which has been linked to anaerobic survival and fitness within a biofilm, is upregulated. Swimming and swarming motility are also elevated in DmftR cells. We further show that MftR is one of several transcription factors which control production of the siderophore malleobactin. MftR binds directly to the promoter driving expression of mbaS, which encodes the extracytoplasmic function sigma factor MbaS that is required for malleobactin production. Malleobactin is a primary siderophore in B. thailandensis as evidenced by reduced siderophore production in mbaS::Tc cells, in which mbaS is disrupted. Expression of mbaS is increased ;5-fold in DmftR cells, and siderophore production is elevated. Under iron-limiting conditions, mbaS expression is increased;150-fold in both wild-type and DmftR cells, respectively, reflecting regula-tion by the ferric uptake regulator (Fur). The mbaS expression profiles also point to repression by a separate, ligand-responsive transcription factor, possibly ScmR. Taken together, these data indicate that MftR controls a number of phenotypes, all of which promote bacterial survival in a host environment.

IMPORTANCE Bacterial pathogens face iron limitation in a host environment. To overcome this challenge, they produce siderophores, small iron-chelating molecules. Uptake of iron-siderophore complexes averts bacterial iron limitation. In Burkholderia spp., malleobactin or related compounds are the primary siderophores. We show here that genes encoding proteins required for malleobactin production in B. thailandensis are under the direct control of the global transcription factor MftR. Repression of gene expression by MftR is relieved when MftR binds xanthine, a purine metabolite present in host cells. Our work therefore identifies a mechanism by which siderophore production may be optimized in a host environment, thus contributing to bacterial fitness.

KEYWORDS ECF sigma factor, Fur, gene regulation, malleobactin, MarR, MbaS, ScmR

Burkholderia thailandensis, which is relatively nonpathogenic to humans, has been used as a model for studying virulence mechanisms of Burkholderia pseudomallei and Burkholderia mallei due to its genetic similarity with these highly pathogenic strains (1). In addition, it has emerged as a source of novel secondary metabolites with antifungal, antitumor, and antibacterial activities (2–5). Expression of genes involved in virulence is often under the control of transcription factors, which belong to the multiple antibiotic resistance (MarR) protein family. B. thailandensis encodes 12 annotated MarR homologs, all of which are conserved in the pathogenic strains (6). MarRs often inhibit transcription by binding to the intergenic region between divergently oriented

Editor Laurie E. Comstock, University of Chicago

Copyright © 2022 American Society for Microbiology. All Rights Reserved.

Address correspondence to Anne Grove, agrove@lsu.edu.

\*Present address: Sudarshan S. Thapa, PPD, part of Thermo Fisher Scientific, Richmond, Virginia, USA.

The authors declare no conflict of interest. Received 17 June 2022 Accepted 1 October 2022 Published 26 October 2022

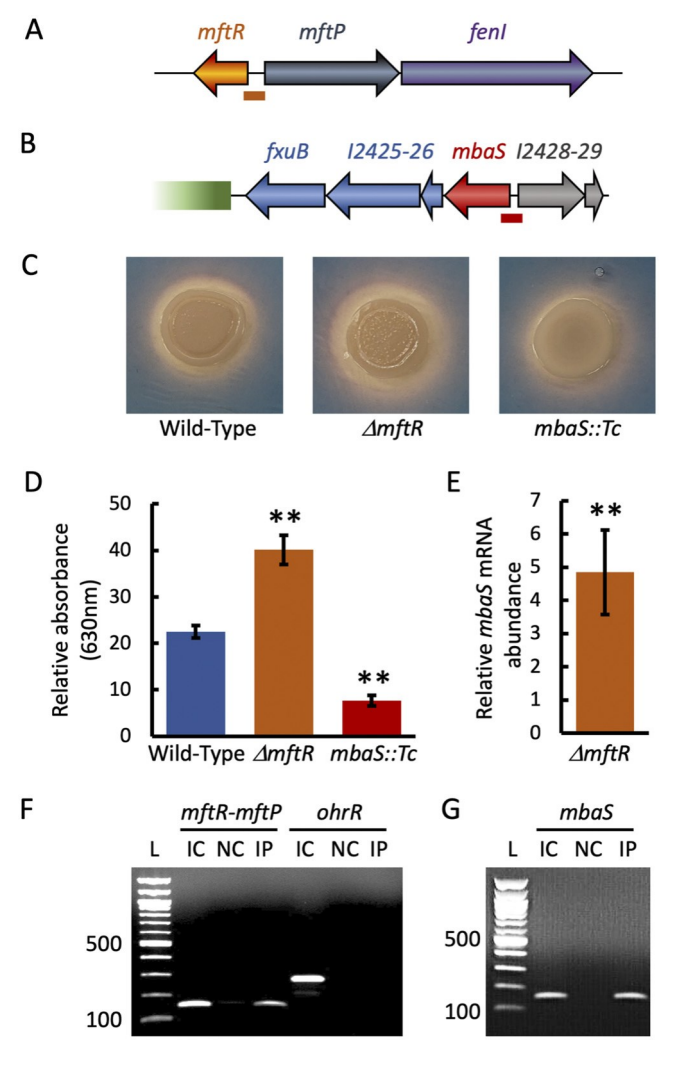


FIG 1 MftR controls mbaS expression and siderophore production. (A) Genomic locus containing mftR (orange) and the mftP-fenI operon. (B) Part of the malleobactin gene cluster. The mbaS gene (red) is part of an operon (blue) with BTH\_I2426 (encoding MbtH-like protein), BTH\_I2425 (syringomycin biosynthesis enzyme), and fxuB (iron compound ABC transporter ATP-binding protein). Additional genes and operons in the mba gene cluster, whose expression depends on MbaS, are not shown (green). The operon divergent to mbaS is annotated as encoding hypothetical proteins (gray). In panels A and B, lines beneath the loci denote amplicons used in ChIP. (C) Siderophore production (orange color) on CAS assay plates. Representative of three biological replicates. (D) Quantitation of siderophore content in culture supernatants. Error bars represent SDs from three biological replicates. (E) Relative mbaS mRNA abundance in DmftR cells. Error bars represent standard deviations from three biological replicates. Transcript levels were calculated using 22DDCT relative to the reference gene and reported relative to wild-type cells. In panels D and E, asterisks denote statistically significant differences compared to wild-type cells based on a Student t test (\*\*,P), 0.001). (F and G) In vivo binding of MftR determined by chromatin immunoprecipitation. PCR products were electrophoresed on 1.5% agarose gels and visualized by ethidium bromide staining for the mftRmftP intergenic region, the ohrR promoter, and the mbaS promoter. Results are representative of three biological replicates. L, 100-bp ladder (at the left, in base pairs); IC, input control; NC, negative control without antibody; IP, immunoprecipitated with anti-FLAG antibody.

genes, one of which encodes the MarR, and they frequently serve as environmental sensors; upon change in environmental conditions such as antibiotic exposure, oxidative stress, and host-pathogen interaction, DNA binding by the MarR is attenuated due to ligand binding or oxidation, resulting in expression of genes associated with enhanced bacterial fitness or virulence (7, 8).

The MarR protein MftR (major facilitator transport regulator) is encoded divergent to an operon encoding a member of the major facilitator superfamily of transport proteins (MftP) and the glycosyl hydrolase-like protein Fenl (Fig. 1A). MftR serves as a global regulator in

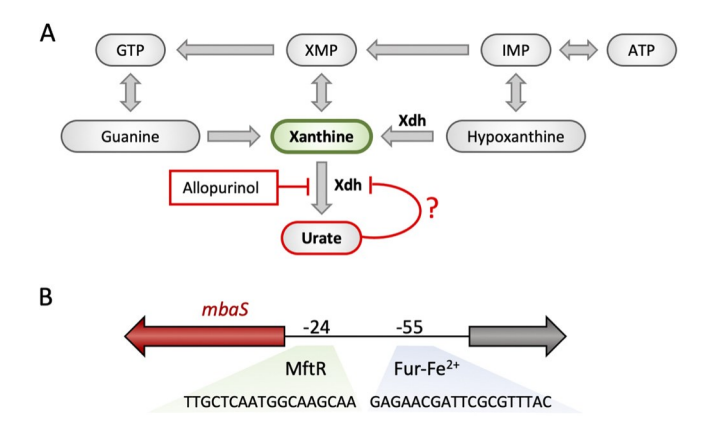


FIG 2 Role of purine metabolites in controlling mbaS expression. (A) Overview of purine salvage (intermediate steps omitted for clarity). Xanthine dehydrogenase (Xdh) converts hypoxanthine to xanthine and xanthine to urate; the latter diverts purines away from the salvage pathway. Allopurinol inhibits Xdh, resulting in reduced production of urate and accumulation of xanthine. Urate may also inhibit Xdh. (B) The mbaS promoter is predicted to include binding sites for MftR and Fur. Positions of predicted sites are indicated relative to the translational start of mbaS.

B. thailandensis where it generally functions as a repressor, with 331 genes upregulated in an mftR disruptant strain, including mftP-fenl and numerous biosynthetic gene clusters involved in secondary metabolite production (2, 5). Urate and xanthine are ligands for MftR, and their binding elicits a conformational change in the protein, which attenuates DNA binding (5, 9–11). Both urate and xanthine are products of xanthine dehydrogenase (Xdh) (Fig. 2A), which participates both in normal purine metabolism and in production of reactive oxygen species (ROS) in response to infection, and urate concentrations of .200 mM have been reported in nonprimate mammalian infection models (12–14). In humans, however, normal concentrations of urate are much higher than in other mammals, with ; 300 mM urate reported in blood (15); the higher basal level of urate is most likely due to the evolutionary loss of uricase activity in primates (16). By comparison, normal levels of xanthine in humans typically do not exceed 1 mM (15), but xanthine (and urate) has been shown to accumulate in plant models of infection (17). Thus, MftR, whose affinity for urate and xanthine is physiologically relevant ( $K_{\rm d}$  [dissociation constant] of ; 6 mM) (9, 10), is poised to sense urate and xanthine upon infection of both mammalian and plant hosts.

While B. thailandensis is relatively nonpathogenic, genes encoding proteins required for synthesis of virulence factors such as secondary metabolites are conserved (18). The cytotoxic polyketide malleilactone, for example, which is required for virulence in B. pseudomallei, is also produced in B. thailandensis (19, 20); genes encoding proteins involved in its synthesis are repressed by MftR, and expression is induced on addition of urate and xanthine (5, 11). We report here that MftR also participates directly in controlling siderophore production. Iron is abundant, yet its bioavailability is low because Fe<sup>31</sup> is poorly soluble and bound to host proteins such as transferrin and lactoferrin (21). Bacteria therefore produce siderophores, small high-affinity metal-chelating molecules, which are critical for iron uptake within the iron-limited host environment (22).

Burkholderia spp. encode more than one type of siderophore, of which ornibactin is considered the most important among members of the Burkholderia cepacia complex (Bcc), while the structurally related malleobactins are produced by members of the Burkholderia pseudomallei complex (Bpc), to which B. thailandensis belongs (23, 24). The ornibactin and malleobactin biosynthetic gene clusters are similar, and production of these siderophores requires an extracytoplasmic function (ECF) sigma factor (named OrbS in B. cenocepacia and MbaS in B. pseudomallei) (25–28). Part of the B. thailandensis mba locus comprising the genes encoding proteins essential for production and transport of malleobactin is shown in Fig. 1B, illustrating that mbaS (red) is part of an operon with three downstream genes (blue); production of MbaS subsequently directs the transcription of other genes and operons within the mba gene cluster (green) (26). We report here that B. thailandensis mbaS

TABLE 1 Primers used for qRT-PCR

Primer	Sequence (59 to 39)
mbaS forward	TCGAGAACACCTACCACGC
mbaS reverse	CGTCGCGGACCATCAAAT
arcA forward	TCCCAAGCCATCCCTGAAG
arcA reverse	CAGGTTGTGCATCTCGAGC
hgprt forward	CGAGAAGAAGCCCTCCACAT
hgprt reverse	TCGAACTCGAGCGGGAAATC

(BTH\_12427) is directly controlled by MftR. Combined with regulation by iron limitation, our data suggest regulatory mechanisms which ensure optimal mba expression in an iron-limited host environment. Consistent with a role for MftR in repression of virulence genes, we also show that an mftR disruptant strain is more virulent as indicated by decreased survival of Caenorhabditis elegans and increased maceration of onion tissue.

## **RESULTS**

The B. thailandensis mba gene cluster encodes proteins involved in primary siderophore production. MbaS has been reported to be essential for malleobactin production in B. pseudomallei (26), and the malleobactin biosynthetic gene cluster (mba) is conserved and functional in B. thailandensis (24) (Fig. 1B). The first gene in this cluster, mbaS, is predicted to be in an operon with three downstream genes (BTH\_I2424-2426; blue), and remaining genes and operons within the mba gene cluster (green) depend on MbaS for expression (26). In B. pseudomallei, no malleobactin is produced in cells carrying a nonpolar deletion of mbaS, and no expression of a separate mba operon was observed (26). The inferences from these experiments are that the genes located downstream of mbaS do not participate in controlling expression of other mba operons and that deletion of mbaS is sufficient to eliminate malleobactin production.

Notably, none of the mba genes encode an anti-sigma factor, which is frequently required to control activity of an ECF sigma factor (29). This suggests that MbaS activity is instead under transcriptional control. To address this question, we created an mbaS disruptant strain (mbaS::Tc); note that disruption of the mbaS coding region is polar and expected also to disrupt expression of BTH 12424-2426. Production of siderophore was assessed using the chrome azurol S (CAS) assay in which chelation of iron by siderophores causes release of the orange CAS dye from a blue Fe-CAS-hexadecyltrimethylammonium bromide complex, resulting in an orange halo surrounding colonies on a blue agar plate and a color change that can be quantitated spectrophotometrically. As seen in Fig. 1C and D, the amount of siderophore produced in the mbaS::Tc strain was reduced compared to that in the wild type (WT), as expected, verifying that the B. thailandensis mba gene cluster encodes proteins involved in synthesis of a primary siderophore. In B. pseudomallei, MbaS is essential for malleobactin production; however, cells deleted for mbaS produce the alternate siderophore pyochelin (26). Since the pyochelin biosynthetic gene cluster is conserved in B. thailandensis, we surmise that residual siderophore produced in our mbaS::Tc strain is pyochelin.

MftR binds mbaS directly. A genome-wide transcriptome analysis previously showed an upregulation of B. thailandensis mbaS in an mftR disruption strain (5). We therefore compared siderophore production levels between the wild type and the DmftR strain and found that the DmftR strain produced more siderophore than did the wild type (Fig. 1C and D). We also verified upregulation of mbaS in the DmftR strain using reverse transcription-quantitative PCR (qRT-PCR) (primers shown in Table 1) and found almost 5-fold-increased expression (Fig. 1E), which is very consistent with the 4.6-fold increase seen by transcriptome sequencing (RNA-seq); the increased mbaS expression correlates with comparably increased expression of all genes in the mba gene cluster (5). The gene expression analysis along with the CAS assay indicates that MftR represses mbaS expression and thereby attenuates siderophore production.

To determine if mbaS is directly regulated by MftR, a chromatin immunoprecipitation (ChIP) assay (primers shown in Table 2) was performed using a previously characterized

TABLE 2 Primers used for ChIP

Primer	Sequence (59 to 39)
mftP-mftR inter forward	GAGCTGCGCGATCCATTAAC
mftP-mftR inter reverse	TGCAGGAGAATTAAGCATGGG
mbaS upstream forward	ATGATCGACGAGCGAAGTG
mbaS upstream reverse	GAGGATCGGTAACGGTTTTG
ohrR upstream forward	GGTCGTCTCCCATCGTTTC
ohrR upstream reverse	GTCGTTCATGGCGAGATTTTC

strain expressing genomic, C-terminally FLAG-tagged MftR (11). For ChIP, the intergenic region between mftR and the divergently oriented gene mftP to which MftR binds in vitro (Fig. 1A) (9, 10) was used as the positive control, and we verified MftR binding to this region in vivo (Fig. 1F). As a control for specificity, a negative control using the ohrR upstream region to which the unrelated transcription factor OhrR binds (30) was used, and no MftR binding was detected. The ability of MftR to bind upstream of mbaS was tested by amplifying a fragment comprising 128 bp upstream of mbaS and part of the coding region, and MftR was found to bind this region (Fig. 1G). Examination of this sequence identifies a possible binding site for MftR centered 24 bp upstream of the mbaS start codon (Fig. 2B). Our ChIP data are consistent with the gene expression analy-sis and siderophore production, supporting the interpretation that MftR binds upstream of mbaS and directly represses its expression.

Regulation of mbaS expression. While the genome-wide transcriptomics data showed comparable upregulation of all genes in the mba gene cluster on disruption of mftR, addition of the MftR ligand urate (5 mM) unexpectedly had little effect on mba gene expression during exponential growth (5). It was also reported that when B. thailandensis is grown to stationary phase in the presence of trimethoprim (12 h), expression of a number of biosynthetic gene clusters is induced, such as the malleilactone biosynthetic gene cluster, which is also directly repressed by MftR. However, expression of the mba gene cluster is not increased under these conditions; instead, it is decreased; the relevance of this observation is that addition of trimethoprim to exponentially growing cultures leads to accumulation of the MftR ligand xanthine (along with other metabolic changes) (11, 20). Evidently, while absence of MftR results in elevated mbaS expression (Fig. 1E), the presence of the MftR ligand urate or xanthine does not.

The B. pseudomallei mbaS promoter contains a Fur-box, the binding site for the global transcriptional regulator Fur (ferric uptake regulator) (26). Fe<sup>21</sup> functions as a corepressor, allowing Fur-Fe<sup>21</sup> to repress genes involved in iron uptake (31). The B. thailandensis mbaS promoter features a Fur-box centered 55 bp upstream of the annotated start codon (Fig. 2B); this sequence differs from the confirmed B. pseudomallei Fur-box by only 1 bp, strongly suggesting that B. thailandensis mbaS is also controlled by iron limitation. Since urate has been reported to form a coordination complex with Fe<sup>31</sup> (32), we were alert to the possibility of urate inducing an iron-limiting condition, which in turn should relieve repression by Fur. In this scenario, urate would be expected to cause increased mbaS expression, regardless of its function as a ligand for MftR. This expectation was also not borne out by the transcriptomics analysis (5).

To address the perplexing failure of the MftR ligands urate and xanthine to induce increased expression of mbaS, we measured its expression under various conditions. In accord with the expected regulation by Fur, mbaS expression was increased 146-fold in wild-type cells exposed to iron limitation imposed by addition of the strong iron chelator bipyridyl (Fig. 3A). In DmftR cells, which are characterized by an ;5-fold-increased mbaS expression compared to wild type (Fig. 1E), bipyridyl-imposed iron limitation also led to significantly increased mbaS expression (151-fold; Fig. 3B). These observations are consistent with regulation by Fur.

When wild-type cells were grown with 2.5 or 5 mM urate, no statistically significant increase in expression was seen (Fig. 3B). In contrast, addition of urate to DmftR cells resulted in a concentration-dependent increase in mbaS expression; addition of low

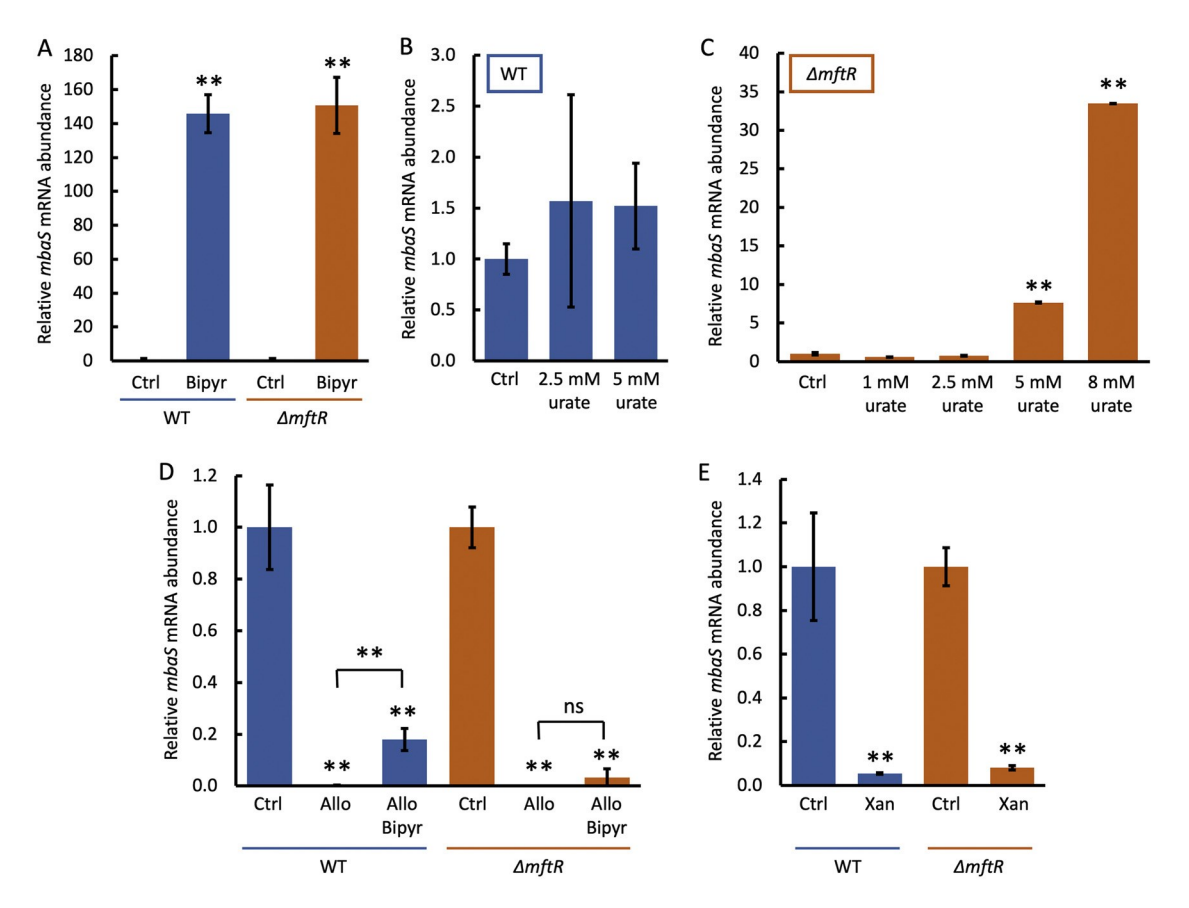


FIG 3 Regulation of mbaS. Relative mbaS mRNA abundance. (A) Wild-type (blue) and DmftR (orange) cells treated with 200 mM bipyridyl (Bipyr) for 30 min. (B) Wild-type cells treated with 2.5 or 5 mM urate for 30 min. (C) DmftR cells treated with different concentrations of urate for 30 min. (D) Wild-type (blue) and DmftR (orange) cells treated with 200 mM bipyridyl (Bipyr) and/or 5 mM allopurinol (Allo) for 30 min. (E) Wild-type (blue) and DmftR (orange) cells treated with 5 mM xanthine (Xan) for 30 min. Transcript levels were calculated using 2<sup>2DDCT</sup> relative to the reference gene and reported relative to control (Ctrl) cells to which an equivalent volume of 0.4 M NaOH (the solvent for ligands) was added. Error bars represent standard deviations from at least three biological replicates. Asterisks denote statistically significant differences compared to control cells based on a Student t test (\*\*, P, 0.001; \*, P, 0.05; ns, not significant).

urate concentrations (1 mM and 2.5 mM) did not lead to a measurable change in mbaS expression, whereas 5 mM urate led to an ;7-fold-increased expression, and addition of 8 mM urate resulted in .40-fold-increased expression (Fig. 3C). We surmise that this increase is due to a modest iron limitation, which is manifest mainly in DmftR cells since the absence of urate binding by MftR may increase the levels of free urate available to bind iron.

Allopurinol inhibits Xdh, the enzyme responsible for converting hypoxanthine to xanthine and xanthine to urate (Fig. 2A). This results in reduced cellular levels of urate and in accumulation of xanthine, and it leads to upregulation of MftR targets such as the malleilactone biosynthetic genes (11). Remarkably, addition of allopurinol to either wild-type or DmftR cells resulted in effectively undetectable mbaS expression (Fig. 3D). Notably, growth of cells with 5 mM xanthine (which leads to lower cellular accumulation of xanthine than does growth with 5 mM allopurinol [11]) also resulted in significantly reduced mbaS expression (Fig. 3E). This suggests that mbaS expression is repressed by a separate transcription factor under these conditions. Indeed, mbaS was previously reported to be repressed by the LysR-type transcriptional regulator (LTTR) ScmR (secondary metabolite regulator). Interestingly, this repression was seen only in stationary phase, as inactivation of scmR has no effect on expression of the mba genes during exponential growth in rich medium (33, 34). LTTRs generally rely on small-molecule cofactors for transcriptional regulation (35). A possible explanation for the ScmR-mediated

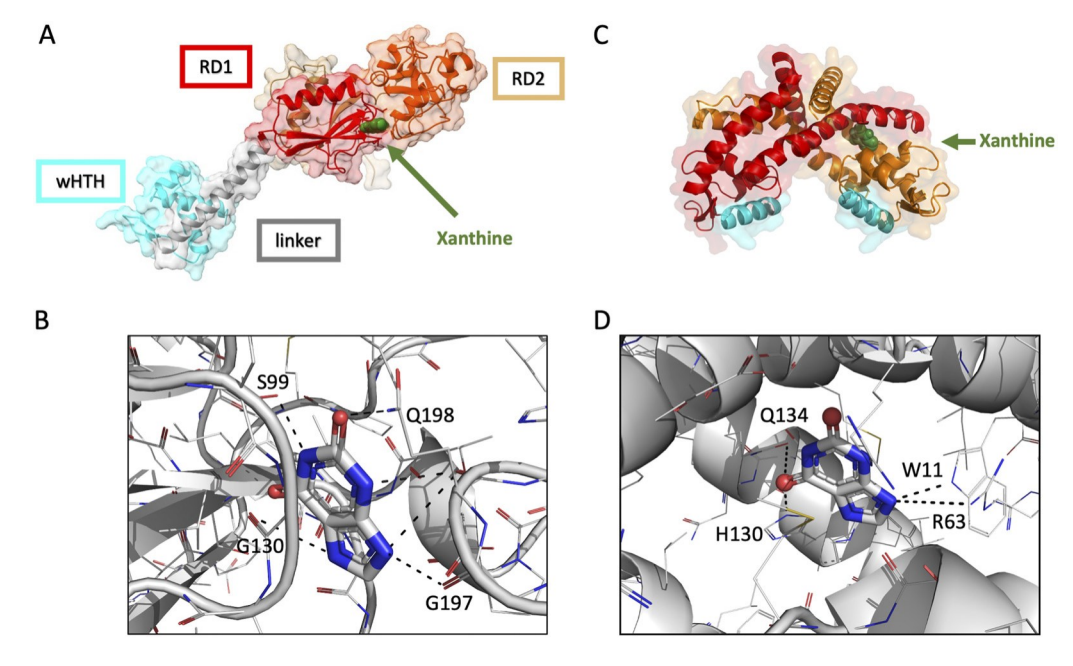


FIG 4 Potential binding pockets for xanthine. (A) Model of ScmR monomer showing the wHTH DNA-binding domain in cyan and a flexible linker (gray) connecting this domain to the ligand-binding domain consisting of two Rossman-like folds (RD1 and RD2, red and orange, respectively). Blind docking predicts binding of xanthine (green) in the interface between RD1 and RD2. (B) Expanded view of predicted binding pocket for xanthine. Xanthine is shown in stick representation; C, gray; N, blue; O, red. The best pose is shown. (C) Model of MftR dimer. Individual subunits are shown in red and orange, except for DNA recognition helices, which are colored cyan. Xanthine (green space-filling representation) is predicted to bind a pocket connecting the wHTH region and the dimer interface. (D) Expanded view of predicted binding pocket for xanthine. The best pose is shown.

repression of mbaS during stationary phase is therefore that its ligand is more abundant under these conditions.

Addition of allopurinol or xanthine to the growth medium leads to elevated cellular levels of xanthine (11), suggesting that conditions which favor significant repression of mbaS are characterized by accumulation of this purine metabolite. One scenario which could explain the marked repression of mbaS is therefore that xanthine functions as a corepressor for ScmR. It should be noted that regulation by ScmR could be indirect, with mbaS regulation depending on a separate transcription factor under ScmR control, but for the sake of argument, direct binding by ScmR to the mbaS promoter is assumed. To assess the hypothesis that xanthine functions to repress mbaS expression, independently of MftR- and Fur-mediated transcriptional control, wild-type and DmftR cells were grown with a combination of bipyridyl and allopurinol. In both wild-type and DmftR cells, this resulted in a net repression compared to untreated cells (Fig. 3D). However, by comparison to cells treated with allopurinol only, addition of bipyridyl still resulted in a significant increase in mbaS expression in wild-type cells, consistent with dissociation of Fur under iron-limiting conditions. For DmftR cells, however, this increase is much less pronounced compared to DmftR cells grown with bipyridyl only (Fig. 3B).

Predicted binding of xanthine to ScmR. LysR-type transcriptional regulators (LTTRs) such as ScmR typically form homotetramers in which each monomer harbors a ligand-binding pocket (35). To predict whether xanthine might function as a corepressor for ScmR, AlphaFold2 was used to model the ScmR monomer (Fig. 4A). As expected, ScmR is comprised of the typical N-terminal winged helix-turn-helix DNA-binding domain (wHTH; cyan) and a C-terminal ligand-binding domain composed of two Rossman-like domains (RD1 and RD2; red and orange); these N- and C-terminal domains were predicted with a high confidence score (predicted local distance difference test [pLDDT] . 90). A flexible linker for which the model confidence was low (70 . pLDDT . 50) connects the N- and C-terminal domains (gray).

Downloaded from https://journals.asm.org/journal/jb on 01 August 2023 by 2600:8807:600:6a0a:2083:a7de:f8b0:d527

This model was used for blind docking with xanthine to assess the likelihood of a direct interaction. The interaction with the lowest Vina score (25.5) and largest cavity size (1,693) was selected. Ligand-binding cavities in LTTRs typically reside in the interface between RD1 and RD2; consistent with this expectation, predicted binding poses for xanthine occupy a pocket in this interface (Fig. 4A and B). The favored pose is characterized by a hydrogen-bonding network comprising the backbone oxygens of Gly197, Gln198, and Gly130 as well as the side chains of Ser99 and Gln198.

By comparison, the dimeric MftR was modeled with high confidence (pLDDT . 94; each subunit in red and orange), reflecting the conserved wHTH DNA-binding regions (recognition helices in cyan) and an extensive dimer interface. Xanthine is predicted to bind in a pocket connecting the DNA-binding and dimerization interfaces (Vina score, 25.7; cavity size, 1,320), as previously reported for the MftR ligand urate (10). Residues predicted to make direct contact with xanthine include Trp11, Arg63, His130, and Gln134; Trp11 was previously shown to be important for protein stability, whereas substitution of Arg63 reduced the affinity for urate by ;10-fold (10). This binding pocket corresponds to the crystallographically determined binding site for urate in the MftR homolog HucR (36).

Increased biofilm formation in DmftR strain. Biofilm is a hallmark of chronic infection as bacteria growing in biofilm not only evade host immune responses but can be resistant to a large number of drugs. Biofilm production also requires availability of iron, with siderophore-deficient cells generally exhibiting reduced biofilm formation (37, 38). We therefore determined if biofilm formation is enhanced in the DmftR strain. After incubation for 72 h, more abundant pellicle biofilm formed at the air-liquid interface in the DmftR strain compared to wild-type cells (Fig. 5A). Quantification using crys-tal violet staining showed an approximately 2-fold-higher production of biofilm in the DmftR strain than in the wild type (Fig. 5B). The DmftR cells exhibit a modestly reduced growth rate, a phenotype that is fully restored to wild-type levels upon complementation with mftR (5), suggesting that increased biofilm formation is not due to an altered growth rate. The level of biofilm formation by the complemented strain DmftR(mftR) was lower than that of DmftR cells and not significantly different from that of wild-type cells.

Cells within the interior of a biofilm community experience a hypoxic environment. Thus, successful establishment of persistent biofilm also requires expression of genes involved in anaerobiosis. Such requirement for anaerobic fitness for virulence and pathogenesis has been reported for Burkholderia spp., and the DmftR strain has been previously reported to grow better under anaerobic conditions than the wild type (5, 39). The arginine deiminase (ADI) pathway has been shown to contribute to anaerobic fitness during biofilm growth, with arcDABC encoding an arginine/ornithine antiporter (ArcD) and enzymes involved in anaerobic degradation of arginine with concomitant production of ATP (40). We found that arcA expression was increased ;3.5-fold in the DmftR strain compared to the wild type, whereas the relative expression level was ;0.5 in DmftR(mftR) cells, consistent with repression by MftR (Fig. 5C). Expression of the arcDABC operon is also increased on addition of urate to wild-type cells, whereas urate has no effect on its expression in DmftR cells (5).

Increased swimming and swarming motility in DmftR cells. Bacterial swimming motility in aqueous media and swarming behavior on hydrated semisolid surfaces play a role in dispersal, avoidance of toxic compounds such as antibiotics, and biofilm formation (41). In order to determine if such flagellum-dependent motility is altered in DmftR cells, swimming and swarming motility assays were performed. Both wild-type and DmftR cells exhibited swimming motility, moving evenly outward from the central inoculation site, whereas swarming patterns were irregular, suggesting alternating cycles of motility and growth and differentiation (Fig. 5D and E). Increased swimming and swarming motility were observed for the DmftR cells compared to wild-type cells as indicated by increased swarming and swimming diameters (Fig. 5D and E, middle panels), and this increased motility was completely reversed by complementation of DmftR with mftR (Fig. 5D and E, right panels). Such increased flagellar motility of DmftR

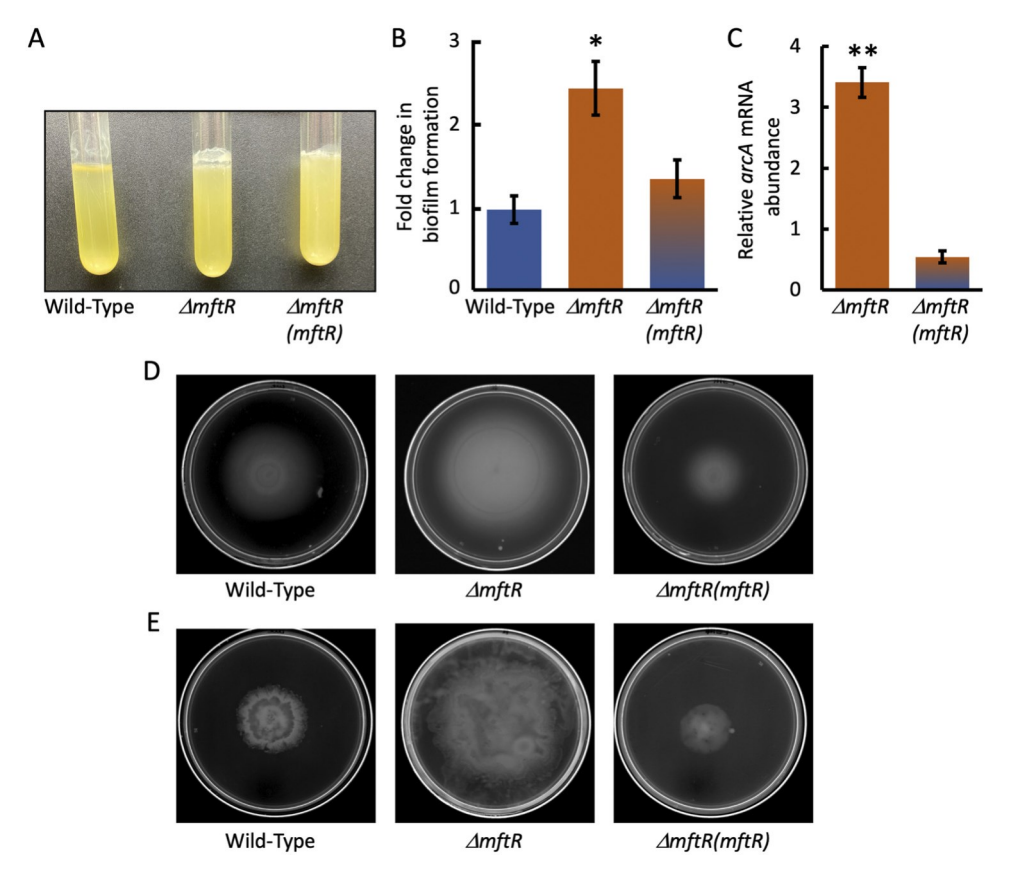


FIG 5 Increased flagellar motility and biofilm formation of DmftR cells. (A) Pellicle biofilm in static cultures of wild-type, DmftR, and DmftR(mftR) cells. Representative of three biological replicates. (B) Relative biofilm formation as determined by crystal violet staining. (C) Relative arcA mRNA abundance in DmftR (n = 6) and DmftR(mftR) (n = 3) cells. Transcript levels were calculated using 2<sup>2DDCT</sup> relative to the reference gene and reported relative to wild-type cells. In panels B and C, error bars represent standard deviations from at least three biological replicates, and asterisks denote statistically significant differences compared to wild-type cells based on a Student t test (\*, P , 0.05; \*\*, P , 0.001). (D) Swimming motility (0.3% agar; imaged after 48 h). (E) Swarming motility (0.5% agar; imaged after 24 h). Data in panels D and E are representative of at least three biological replicates.

cells along with an enhanced ability to tolerate anaerobic conditions would be expected to promote virulence.

DmftR cells are more virulent. The DmftR strain exhibits physiological characteristics generally associated with virulence, including enhanced siderophore production, motility, anaerobic fitness, and biofilm formation. Moreover, MftR directly represses malR; malR encodes an essential activator of the mal gene cluster, which encodes enzymes essential for production of the virulence factor malleilactone (11). We therefore examined virulence of the DmftR strain using Caenorhabditis elegans. Worms were deposited on lawns of wild-type or DmftR B. thailandensis, using the standard Escherichia coli OP50 food source as a reference. Approximately 60% of the C. elegans worms died when coincubated with DmftR cells compared to only 20% death of C. elegans worms that were coincubated with wild-type B. thailandensis; worms were declared dead if insensitive to touch (Fig. 6A).

Several species in the genus Burkholderia cause onion rot, but no such effect has been reported for B. thailandensis (42). To determine if the DmftR strain is also more virulent on a plant host, onion scales were wounded and inoculated with wild-type or DmftR cells. Onion scales inoculated with Luria broth (LB) only showed no deterioration (Fig. 6B and C). In contrast, onion scales inoculated with DmftR cells developed a significantly higher area of maceration than did scales inoculated with wild-type cells. Evidently, the DmftR strain exhibits increased virulence in both C. elegans and plant models.

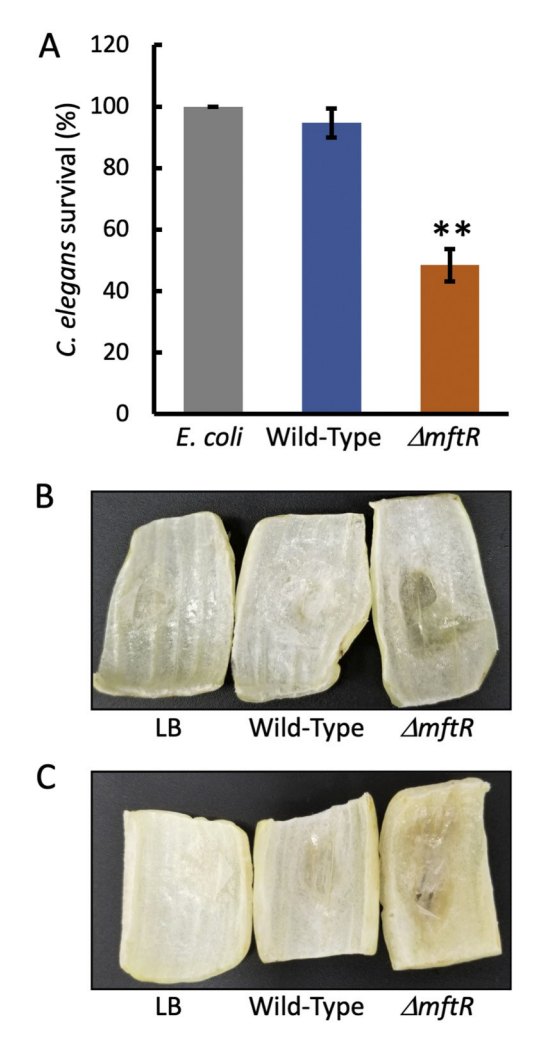


FIG 6 Increased virulence of DmftR cells. (A) Survival of C. elegans coincubated with E. coli OP50 (gray bar), wild-type B. thailandensis (blue bar), or the DmftR strain (orange bar) on NGM plates at room temperature for 24 h (mean 6 SD from three independent experiments). Asterisks indicate statistically significant differences between wild-type and DmftR cells (\*\*, P, 0.001). (B and C) Maceration of onion scales after 72 h of incubation with LB (control), wild-type cells, and DmftR cells. (B) The outermost scale beneath the tunics. (C) The second layer of scales. Representative of three biological replicates.

# **DISCUSSION**

Motility and biofilm formation—phenotypes linked to virulence. Flagellar motility is coupled to the chemotaxis machinery, and it enables bacteria to move toward favorable environments as well as host cells. In the context of a mammalian host, mucosal surfaces are primary sites for the initial host-pathogen interaction, and flagella may participate directly in colonization (43, 44). In B. cenocepacia, for instance, flagella have been reported to play an important role in virulence in a murine agar bead model of infection (45). In cystic fibrosis patients, the lung may become chronically infected with Bcc species such as B. cenocepacia, and analyses of isolates from chronic infections have suggested that the bacteria do not systematically switch to nonmotile phenotypes (as for example observed for Pseudomonas aeruginosa), a characteristic possibly linked to their ability to cause invasive pneumonia (cepacia syndrome) (46). B. thailandensis MftR represses motility as evidenced by increased swimming and swarming motility of DmftR cells (Fig. 5D and E). Since MftR is conserved in Bcc species (6), it is therefore conceivable that the elevated urate concentration characteristic of the mammalian host contributes to maintaining bacterial motility during chronic infection by serving as a ligand for MftR.

Downloaded from https://journals.asm.org/journal/jb on 01 August 2023 by 2600:8807:600:6a0a:2083:a7dc:f8b0:d527

In contrast, in the C. elegans virulence assay in which the worms ingest the bacteria, motility is less likely to be required for virulence (47).

Successful colonization of the host also requires mechanisms to avoid host defenses, including reactive oxygen species (ROS), and antibiotics. One such mechanism is biofilm formation (48). A hypoxic environment is experienced by cells deeper in a biofilm community, and genes involved in anaerobiosis therefore play a critical role in establishment of persistent biofilm (49). Consistent with the enhanced biofilm formation of DmftR cells (Fig. 5A and B), deletion of mftR also promotes growth in an anaerobic environment compared to wild-type cells (5). The observed increase in arcDABC expression in DmftR cells (Fig. 5C) would be expected to promote the ability of DmftR cells to form a persistent biofilm.

Control of siderophore production. For bacteria to survive in a host environment, high-affinity iron acquisition is critical (50). Accordingly, almost all Bcc species produce the siderophore ornibactin, which is required for virulence, while Bpc species synthesize the structurally related malleobactins (23). Fur-mediated regulation by iron limitation was confirmed for B. pseudomallei mbaS and for B. cenocepacia orbS (25, 26), and Fur-mediated regulation of the B. thailandensis mba gene cluster is therefore a strong prediction, which is supported by the presence of a conserved Fur-box and by the significant upregulation of mbaS under conditions of iron limitation (Fig. 3A). The comparable increase in mbaS expression on addition of bipyridyl to either WT or DmftR cells shows that iron-mediated regulation is unrelated to regulation by MftR.

Siderophores are required for survival in an iron-restricted host environment; however, their synthesis and transport are demanding in terms of cellular resources, and their production is therefore under tight control. One level of control is for genes to remain repressed when iron is abundant, a level of regulation executed by Fur (Fig. 3A and Fig. 7A and B). Siderophores such as malleobactin are taken up by high-affinity transporters (27); under conditions of high cell density, the overall siderophore production by the bacterial community may therefore be optimal if mba gene expression by individual cells is reduced compared to that by a more dispersed cell population. Such regulation appears to be performed (directly or indirectly) by ScmR, which has been reported to repress mba genes only in stationary phase (33, 34). Since scmR expression is promoted by quorum sensing, one possibility is that elevated cellular levels of ScmR during stationary phase contribute to more efficient repression.

However, stationary phase is also associated with the stringent response, conditions under which purine salvage is favored over de novo synthesis, and this has been shown to include upregulation of the xdh operon (51, 52). In B. thailandensis, upregulation of xdh correlates with accumulation of xanthine and with upregulation of the malleilac-tone biosynthetic genes, which are under the control of MftR (11). It is therefore con-ceivable that xanthine, which accumulates during the stringent response, acts as a ligand not only for MftR but also for ScmR, resulting in net repression of the mba genes. The reduced expression of mba genes when cells are grown with trimethoprim (which leads to accumulation of xanthine [11, 20]) and the marked repression of mbaS on addition of allopurinol or xanthine are consistent with this scenario (Fig. 3D and E). The observation that mbaS expression is higher in cells grown with both allopurinol and bipyridyl than in cells treated with allopurinol alone (Fig. 3D) suggests that iron-mediated regulation by Fur is unrelated to repression mediated by xanthine.

ScmR is negatively autoregulated; however, increased scmR promoter activity in an scmR mutant strain was only partially complemented with ScmR produced in trans. This was ascribed to an imbalance between overexpressed ScmR and its (unknown) ligand (33). In addition, no autoregulation was seen when reporter construct and ScmR were expressed in E. coli, an outcome that was likewise inferred to be due to insufficient levels of ligand. Together, these observations indicate that ScmR activity is indeed modulated by a ligand. Ligands for LTTRs are often intermediates or products of biosynthetic pathways, which are activated by the LTTR; this creates a feedback loop, which serves to optimize LTTR function (35). Notably, expression of xdhA and

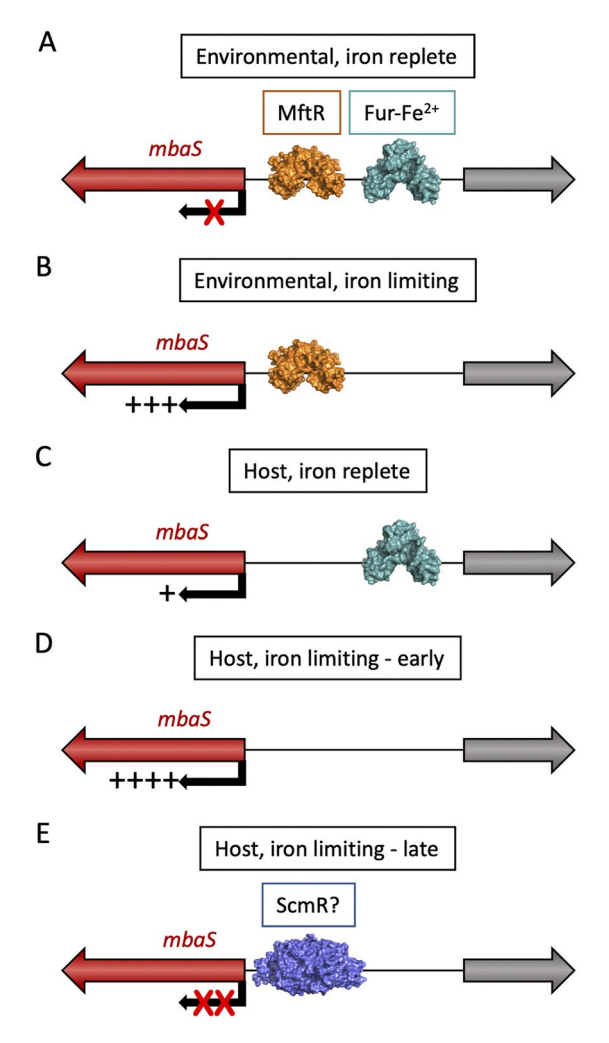


FIG 7 Model for control of mbaS expression. (A) During growth under iron-replete environmental conditions, mbaS is repressed by both Fur-Fe<sup>21</sup> and MftR. (B) Iron limitation leads to dissociation of Fur and elevated expression of mbaS (and in turn the entire mba gene cluster). (C) In a host environment, characterized by elevated urate levels, MftR dissociates, resulting in a modest increase in mbaS expression. (D) In an iron-limited host environment, both Fur and MftR dissociate. (E) Accumulation of xanthine during stringent response may lead to ScmR-mediated repression of mbaS under conditions of high cell density.

xdhB (BTH\_I1408-1409) is more than 6-fold-reduced in an scmR mutant strain compared to WT during exponential growth, suggesting that ScmR activates expression (33). This reflects a direct link between ScmR and the purine salvage pathway.

In cells growing exponentially under iron-replete environmental conditions, mbaS expression is simultaneously repressed by Fur-Fe<sup>21</sup> and MftR, whereas ScmR does not participate (Fig. 7A). It is conceivable that MftR binding precludes ScmR binding, explaining why inactivation of scmR has no effect on mbaS expression under these conditions. Fur is released as a consequence of iron limitation (Fig. 7B), and MftR dissociates when it binds urate or xanthine (Fig. 7C), which accumulates during host infection. This dual regulation by Fur and MftR may therefore ensure that mbaS expression is most sensitively upregulated in an iron-limited host environment (Fig. 7D).

However, uncontrolled expression of mba genes would lead to excess malleobactin production, which is averted due to repression of mbaS by ScmR. The very marked repression of mbaS observed on addition of allopurinol or xanthine (Fig. 3D and E) leads us to predict that ScmR represses mbaS only on binding the corepressor xanthine (while noting that xanthine would also lead to dissociation of MftR [Fig. 7E]). The

TABLE 3 Primers used for creation and verification of mbaS::Tc strain

Primer	Sequence (59 to 39) <sup>a</sup>
Ecf_ko_Fwd	GCTCTAGAGTGAAGCTCGTCGATTTCCC
Ecf_ko_Rev	GCGGTACCCGTCGCGGACCATGAAAT
ECF veri_Fwd	AGACGCTCGTGCATTTCAT
ECF veri_Rev	TTGCGGAGAACTGTGAATGC
pKnock_tc_rev	GAGAACTGTGAATGCGCAAA

aRestriction sites are boldfaced.

observation that mbaS expression is either unaffected or modestly increased on addition of urate (Fig. 3B) further suggests that urate is a ligand only for MftR and not for ScmR. In humans, where levels of both purine metabolites have been measured, levels of urate are much higher than those of xanthine (15). When the bacteria encounter elevated levels of purine metabolites on host invasion, this might create a situation in which urate-bound MftR first abandons the mbaS promoter, perhaps along with dissociation of Fur as a consequence of iron limitation, leading to increased expression of mba genes. Since elevated urate levels, imposed by ROS production by Xdh, may in turn inhibit Xdh (as reported for the mammalian Xdh [53]) (Fig. 2A), xanthine levels may rise further, resulting in mbaS repression by xanthine-bound ScmR to curtail malleobactin production.

#### MATERIALS AND METHODS

Growth media and strains. Bacterial cells were grown in Luria broth (LB) medium. The C. elegans assay was performed on 60-mm nematode growth medium (NGM) plates. C. elegans (Bristol strain N2) worms were maintained at room temperature on NGM with E. coli OP50 as the food source. The B. thailandensis E264 strain was obtained from the American Type Culture Collection (ATCC). The mftR disruptant strain obtained by Campbell-type plasmid insertion was previously described and named the DmftR strain (5). Genetic complementation was achieved by cloning mftR with its promoter into plasmid pBBR1-MCS5, which confers gentamicin resistance, followed by conjugative plasmid transfer, as described previously (5). The DmftR(mftR) complemented strain was grown with 250 mg mL<sup>21</sup> gentamicin.

Construction of an mbaS disruptant strain. Disruption of mbaS (BTH\_I2427) was achieved by plasmid insertion (5). A 346-bp fragment of the mbaS open reading frame was amplified using primers Ecf\_ko\_Fwd and Ecf\_ko\_Rev (Table 3). The PCR product was cloned into the suicide vector pKNOCK-Tc (54). The construct was transformed into E. coli SM10I pir cells. For creating the mbaS disruptant strain, mating was performed by mixing the overnight culture of SM10I pir with B. thailandensis at a 2:1 ratio (donor to recipient). The mixture was washed twice with 1 mL of LB and resuspended in 60 mL of LB. The mixture was then spotted on an LB plate and incubated at 37°C for 12 h. The mating mixture was scraped off and resuspended in 1 mL of LB. Serial dilutions (up to 10<sup>25</sup>) of the culture were made, and transformants were selected on LB agar plates containing 80 mg/mL of tetracycline and 15 mg/mL of gentamicin. To verify the gene disruption, PCR was conducted using ECF\_veri\_Fwd and pKnock\_tc\_rev primers. The resulting strain was named the mbaS::Tc strain to reflect that the inserted plasmid confers tetracycline resistance.

Pellicle and biofilm formation. For determination of pellicle and biofilm formation, an overnight culture of wild-type, DmftR, and DmftR(mftR) strains was diluted to 1 unit of optical density (OD), and 30 mL was added to 3 mL of LB medium in a plastic tube. The culture was kept stationary at 37°C for 72 h. After the incubation, pellicle formation was visually observed. For quantitation of biofilm formation, the medium was gently removed, and the tubes were washed with water to remove planktonic cells. One milliliter of 0.1% crystal violet was added to the tube and gently distributed evenly across the surface. After 15 min of incubation, excess crystal violet was decanted, and the tubes were washed twice with water. Tubes were then allowed to air dry, and 1 mL of dimethyl sulfoxide (DMSO) was added to dissolve the crystal violet stain. The solution was incubated at room temperature for 15 min, and OD was measured at 560 nm. Data represent three independent biological samples, each measured in duplicate.

Swarming and swimming assays. For the swarming assay, agar plates (0.5% [wt/vol] Difco Bacto agar, 8 g/L of Difco nutrient broth, 5 g/L of glucose) were prepared and allowed to dry at room temperature for 8 to 10 h. An overnight culture was diluted to an OD at 600 nm (OD $_{600}$ ) of ;1, and 1 mL of the culture was spotted at the center of the plate, which was incubated at 37°C for 24 h. Swimming assays were conducted similarly, except that the agar plates were composed of 0.3% (wt/vol) Difco Bacto agar, 10 g/L of tryptone, and 5 g/L of NaCl. For swimming assays, plates were incubated for 48 h. Results are representative of at least three biological replicates.

CAS assay. Siderophore production was detected by the chrome azurol S (CAS) assay (5). Briefly, cells grown overnight were diluted to an  $OD_{600}$  of ;0.6, and pellets were collected by centrifugation at 13,000 g for 1.5 min. The supernatant was discarded, cells were resuspended in 20 mL of LB, and 10 mL of the cells was spotted at the center of the CAS plate. Plates were incubated at 37°C for 48 h. For quantitation, the filtered supernatant was incubated with CAS reagents, and the absorbance was

Downloaded from https://journals.asm.org/journal/jb on 01 August 2023 by 2600:8807:600:6a0a:2083:a7dc:f8b0:d527

measured at 630 nm and reported relative to a reference containing LB, as described previously (5). Results represent three biological replicates and are presented as mean 6 standard deviation (SD).

qRT-PCR. An overnight culture of B. thailandensis was diluted 1:100 and subcultured in 50 mL LB medium and grown until  $OD_{600}$  reached ;0.6. One milliliter of the cell culture was pelleted, washed twice with autoclaved diethyl pyrocarbonate (DEPC)-treated water, and stored at 280°C. For assessing the effect of ligands, cells were grown in 2 YT (16 g/L tryptone, 10 g/L yeast extract, 5 g/L NaCl; adjusted to pH 7.0); xanthine was added to a final concentration of 5.0 mM and urate was added to a final concentration of 1.0, 2.5, 5.0, or 8.0 mM at an  $OD_{600}$  of ; 0.4, and cells were harvested at an  $OD_{600}$  of ;0.6. Bipyridyl was added to a final concentration of 200 mM, and allopurinol was added to a final concentration of 5.0 mM. All reagents were dissolved in 0.4 M NaOH, and an equivalent volume of 0.4 M NaOH was added to control cultures. RNA was extracted utilizing the Monarch total RNA miniprep kit (New England Biolabs, Ipswich, MA) according to the manufacturer's protocol. RNA was electrophoresed on agarose gels to ascertain integrity, and PCR was performed to verify absence of genomic DNA contamination. For measuring gene expression, one-step quantitative PCR (qPCR) was performed using Luna one-step universal master mix (New England Biolabs). Data represent means (6SDs) from biologi-cal triplicates (each determined from technical triplicates) using the comparative threshold cycle (C<sub>T</sub>) method (2<sup>2DDCT</sup>) for which hgprt (BTH\_I1148) was used as a reference gene. The C<sub>T</sub> values for hgprt were constant under the conditions used for these experiments.

Molecular docking of xanthine to ScmR and MftR. The amino acid sequences of secondary metabolite regulator (ScmR; BTH\_11403) and MftR (BTH\_12391) were downloaded in FASTA format from the Burkholderia Genome Database (https://www.burkholderia.com) (55). The sequences were used to predict the three-dimensional (3D) structure with AlphaFold2 using the GitHub Colaboratory Notebook server (https://github.com/sokrypton/ColabFold) (56). The multiple sequence alignments were performed using MMseqs2 using the default parameters. Five models were generated and ranked based on predicted local distance difference test (pLDDT) score per position, and the models with the highest predicted pLDDT score were chosen. The structure of xanthine was downloaded from the PubChem database (https://pubchem.ncbi.nlm.nih.gov) (57) as an sdf file. CB-Dock (which performs the molecular docking using AutoDock Vina; http://clab.labshare.cn/cb-dock/php/index.php) (58) was used to predict the best possible ScmR and MftR binding pockets for xanthine. On the basis of the Vina score, cavity size, and ligand-binding positions, the best docked poses for xanthine were selected. Image files were generated using ChimeraX1.3 (59).

ChIP. The strain expressing FLAG-tagged MftR was described previously (11). An overnight culture of B. thailandensis MftR-FLAG was diluted 1:100 in 50 mL LB. Once the cells reached an OD<sub>600</sub> of ;0.6, 1% formaldehyde was added to the flask, which was placed on a shaker for 16 min to allow cross-linking to occur. The cell culture was centrifuged at 3,500 g at 4°C for 8 min, and the supernatant was discarded. Cell pellets were washed twice by adding 20 mL of phosphate-buffered saline (PBS) followed by another wash with 5 mL of PBS and centrifuging at 3,500 g for 5 min. Finally, the pellets were resuspended in 1 mL of PBS and the supernatant was removed after centrifuging at 13,000 g for 1 min. Cell pellets were stored at 280°C. Chromatin immunoprecipitation (ChIP) was performed as previously described with some modifications (60). Cells were suspended in 1 mL of lysis buffer with protease inhibitor cocktail and placed on ice for 1 h. Genomic DNA was sheared by sonicating 5 times at 35% output using 10-s pulses at 1-min intervals. Cell/cell debris-free lysate was collected by centrifugation at 13,000 g at 4°C for 12 min and transferred to a clean tube. The lysate was centrifuged for another 3 min, and the final lysate was collected. The lysate was precleared using protein G-Sepharose beads (GE Healthcare) to reduce nonspecific binding to the beads. For immunoprecipitation, 5 mL of anti-FLAG (M2; MilliporeSigma, Burlington, MA) antibodies was used. Eluted DNA from ChIP samples or input DNA was analyzed by PCR (primer sequences shown in Table 2). PCR products were electrophoresed on 1.5% agarose gels containing ethidium bromide. Signal intensities from PCR data were quantified from the TIFF images by using ImageJ software. Experiments were performed in triplicate.

C. elegans survival assay. For assessment of virulence, 10 mL of E. coli OP50 (control), wild-type B. thailandensis, and DmftR strains grown overnight were spotted on NGM plates. Plates were incubated at 37°C for 24 h. After equilibration of the plates at room temperature for 12 h, 10 to 12 C. elegans worms were added to the plates and left for 12 h at room temperature before being checked for survival. Worms were observed under a light microscope (Olympus SZ-ST) for their ability to maintain body posture and sensitivity to touch. Worms that were completely insensitive to touch and had lost their ability to maintain normal body posture were declared dead. The percentage of surviving worms was calcu-lated as survival (%) = (live worms/total worms used) 100. The experiment was performed with three separate biological samples, each in technical triplicate.

Onion tissue maceration. Onion tissue maceration was performed as previously described (42). Yellow onions (Allium cepa) commercially available in grocery stores were utilized for the pathogenicity experiment. The outer tunics were removed completely before cutting the bulb vertically with a sterile razor to get long cylindrical scales. These scales were further cut to get uniform size. About 10 autoclaved napkins were placed in a plastic container and sprayed with autoclaved water to create a moist environment before introducing the onion slices. For this assay, wild-type or DmftR cells were grown overnight (18 to 20 h) on LB plates. Cells were then resuspended in LB to get 10<sup>10</sup> CFU/mL of culture. The inner surface of individual scales was scraped gently with a sterile pipette tip to remove the outer epidermal layer and create a wound. Ten microliters of bacterial culture (10<sup>7</sup> CFU/mL) was inoculated into the wound. The onion scales were incubated at 30°C for 72 h. The degree of maceration was visually inspected, and images of individual slices were taken. Cell-free medium (LB only) was used as a control. The experiment was performed with three biological samples of each strain.

## **ACKNOWLEDGMENTS**

Worms were generously provided by R. Lu.

This work was supported by the National Science Foundation (MCB-1714219 to A.G.).

We declare that there is no conflict of interest.

#### **REFERENCES**

- Yu Y, Kim HS, Chua HH, Lin CH, Sim SH, Lin D, Derr A, Engels R, DeShazer D, Birren B, Nierman WC, Tan P. 2006. Genomic patterns of pathogen evolution revealed by comparison of Burkholderia pseudomallei, the causative agent of melioidosis, to avirulent Burkholderia thailandensis. BMC Microbiol 6:46. https://doi.org/10.1186/1471-2180-6-46.
- Thapa SS, Grove A. 2019. Do global regulators hold the key to production of bacterial secondary metabolites? Antibiotics (Basel) 8:160. https://doi.org/10.3390/antibiotics8040160.
- 3. Klaus JR, Coulon PML, Koirala P, Seyedsayamdost MR, Deziel E, Chandler JR. 2020. Secondary metabolites from the Burkholderia pseudomallei complex: structure, ecology, and evolution. J Ind Microbiol Biotechnol 47:877–887. https://doi.org/10.1007/s10295-020-02317-0.
- Seyedsayamdost MR. 2014. High-throughput platform for the discovery of elicitors of silent bacterial gene clusters. Proc Natl Acad Sci U S A 111: 7266–7271. https://doi.org/10.1073/pnas.1400019111.
- Gupta A, Bedre R, Thapa SS, Sabrin A, Wang G, Dassanayake M, Grove A. 2017. Global awakening of cryptic biosynthetic gene clusters in Burkholderia thailandensis. ACS Chem Biol 12:3012–3021. https://doi.org/10 .1021/acschembio.7b00681.
- Gupta A, Pande A, Sabrin A, Thapa SS, Gioe BW, Grove A. 2019. MarR family transcription factors from Burkholderia species: hidden clues to control of virulence-associated genes. Microbiol Mol Biol Rev 83:e00039-18. https://doi.org/10.1128/MMBR.00039-18.
- Deochand DK, Grove A. 2017. MarR family transcription factors: dynamic variations on a common scaffold. Crit Rev Biochem Mol Biol 52:595–613. https://doi.org/10.1080/10409238.2017.1344612.
- Beggs GA, Brennan RG, Arshad M. 2020. MarR family proteins are important regulators of clinically relevant antibiotic resistance. Protein Sci 29: 647–653. https://doi.org/10.1002/pro.3769.
- 9. Grove A. 2010. Urate-responsive MarR homologs from Burkholderia. Mol Biosyst 6:2133–2142. https://doi.org/10.1039/c0mb00086h.
- Gupta A, Grove A. 2014. Ligand-binding pocket bridges DNA-binding and dimerization domains of the urate-responsive MarR homologue MftR from Burkholderia thailandensis. Biochemistry 53:4368–4380. https://doi.org/10.1021/bi500219t.
- Thapa SS, Grove A. 2021. Impaired purine homeostasis plays a primary role in trimethoprim-mediated induction of virulence genes in Burkholderia thailandensis. Mol Microbiol 115:610–622. https://doi.org/10.1111/mmi.14626.
- Martin HM, Hancock JT, Salisbury V, Harrison R. 2004. Role of xanthine oxidoreductase as an antimicrobial agent. Infect Immun 72:4933–4939. https://doi.org/10.1128/IAI.72.9.4933-4939.2004.
- Segal BH, Sakamoto N, Patel M, Maemura K, Klein AS, Holland SM, Bulkley GB. 2000. Xanthine oxidase contributes to host defense against Burkholderia cepacia in the p47(phox-/-) mouse model of chronic granulomatous disease. Infect Immun 68:2374–2378. https://doi.org/10.1128/IAI.68.4 2374-2378.2000.
- Crane JK, Naeher TM, Broome JE, Boedeker EC. 2013. Role of host xanthine oxidase in infection due to enteropathogenic and Shiga-toxigenic Escherichia coli. Infect Immun 81:1129–1139. https://doi.org/10.1128/IAI .01124-12.
- 15. Wishart DS, Feunang YD, Marcu A, Guo AC, Liang K, Vazquez-Fresno R, Sajed T, Johnson D, Li C, Karu N, Sayeeda Z, Lo E, Assempour N, Berjanskii M, Singhal S, Arndt D, Liang Y, Badran H, Grant J, Serra-Cayuela A, Liu Y, Mandal R, Neveu V, Pon A, Knox C, Wilson M, Manach C, Scalbert A. 2018. HMDB 4.0: the human metabolome database for 2018. Nucleic Acids Res 46:D608–D617. https://doi.org/10.1093/nar/gkx1089.
- Kratzer JT, Lanaspa MA, Murphy MN, Cicerchi C, Graves CL, Tipton PA, Ortlund EA, Johnson RJ, Gaucher EA. 2014. Evolutionary history and metabolic insights of ancient mammalian uricases. Proc Natl Acad Sci U S A 111:3763–3768. https://doi.org/10.1073/pnas.1320393111.
- 17. Ma X, Wang W, Bittner F, Schmidt N, Berkey R, Zhang L, King H, Zhang Y, Feng J, Wen Y, Tan L, Li Y, Zhang Q, Deng Z, Xiong X, Xiao S. 2016. Dual and opposing roles of xanthine dehydrogenase in defense-

- associated reactive oxygen species metabolism in Arabidopsis. Plant Cell 28:1108–1126. https://doi.org/10.1105/tpc.15.00880.
- 18. Sahl JW, Vazquez AJ, Hall CM, Busch JD, Tuanyok A, Mayo M, Schupp JM, Lummis M, Pearson T, Shippy K, Colman RE, Allender CJ, Theobald V, Sarovich DS, Price EP, Hutcheson A, Korlach J, LiPuma JJ, Ladner J, Lovett S, Koroleva G, Palacios G, Limmathurotsakul D, Wuthiekanun V, Wongsuwan G, Currie BJ, Keim P, Wagner DM. 2016. The effects of signal erosion and core genome reduction on the identification of diagnostic markers. mBio 7: e00846-16. https://doi.org/10.1128/mBio.00846-16.
- Klaus JR, Deay J, Neuenswander B, Hursh W, Gao Z, Bouddhara T, Williams TD, Douglas J, Monize K, Martins P, Majerczyk C, Seyedsayamdost MR, Peterson BR, Rivera M, Chandler JR. 2018. Malleilactone is a Burkholderia pseudomallei virulence factor regulated by antibiotics and quorum sensing. J Bacteriol 200:e00008-18. https://doi.org/10.1128/JB.00008-18.
- Li A, Mao D, Yoshimura A, Rosen PC, Martin WL, Gallant E, Wuhr M, Seyedsayamdost MR. 2020. Multi-omic analyses provide links between low-dose antibiotic treatment and induction of secondary metabolism in Burkholderia thailandensis. mBio 11:e03210-19. https://doi.org/10.1128/ mBio.03210-19.
- Page MGP. 2019. The role of iron and siderophores in infection, and the development of siderophore antibiotics. Clin Infect Dis 69:S529–S537. https://doi.org/10.1093/cid/ciz825.
- Ellermann M, Arthur JC. 2017. Siderophore-mediated iron acquisition and modulation of host-bacterial interactions. Free Radic Biol Med 105:68–78. https://doi.org/10.1016/j.freeradbiomed.2016.10.489.
- Butt AT, Thomas MS. 2017. Iron acquisition mechanisms and their role in the virulence of Burkholderia species. Front Cell Infect Microbiol 7:460. https://doi.org/10.3389/fcimb.2017.00460.
- Franke J, Ishida K, Hertweck C. 2015. Plasticity of the malleobactin pathway and its impact on siderophore action in human pathogenic bacteria. Chemistry 21:8010–8014. https://doi.org/10.1002/chem.201500757.
- Agnoli K, Lowe CA, Farmer KL, Husnain SI, Thomas MS. 2006. The ornibactin biosynthesis and transport genes of Burkholderia cenocepacia are regulated by an extracytoplasmic function sigma factor which is a part of the Fur regulon. J Bacteriol 188:3631–3644. https://doi.org/10.1128/JB..188.10.3631-3644.2006.
- Alice AF, Lopez CS, Lowe CA, Ledesma MA, Crosa JH. 2006. Genetic and transcriptional analysis of the siderophore malleobactin biosynthesis and transport genes in the human pathogen Burkholderia pseudomallei K96243. J Bacteriol 188:1551–1566. https://doi.org/10.1128/JB.188.4.1551 -1566.2006.
- Grove A. 2022. Extracytoplasmic function sigma factors governing production of the primary siderophores in pathogenic Burkholderia Species. Front Microbiol 13:851011. https://doi.org/10.3389/fmicb.2022.851011.
- Butt AT, Banyard CD, Haldipurkar SS, Agnoli K, Mohsin MI, Vitovski S, Paleja A, Tang Y, Lomax R, Ye F, Green J, Thomas MS. 2022. The Burkholderia cenocepacia iron starvation sigma factor, OrbS, possesses an on-board iron sensor. Nucleic Acids Res 50:3709–3726. https://doi.org/10.1093/nar/gkac137.
- Staron A, Sofia HJ, Dietrich S, Ulrich LE, Liesegang H, Mascher T. 2009. The third pillar of bacterial signal transduction: classification of the extracytoplasmic function (ECF) sigma factor protein family. Mol Microbiol 74: 557–581. https://doi.org/10.1111/j.1365-2958.2009.06870.x.
- Pande A, Veale TC, Grove A. 2018. Gene regulation by redox-sensitive Burkholderia thailandensis OhrR and its role in bacterial killing of Caenorhabditis elegans. Infect Immun 86:e00322-18. https://doi.org/10.1128/IAI.00322-18.
- Fillat MF. 2014. The FUR (ferric uptake regulator) superfamily: diversity and versatility of key transcriptional regulators. Arch Biochem Biophys 546:41–52. https://doi.org/10.1016/j.abb.2014.01.029.
- Davies KJ, Sevanian A, Muakkassah-Kelly SF, Hochstein P. 1986. Uric acidiron ion complexes. A new aspect of the antioxidant functions of uric acid. Biochem J 235:747–754. https://doi.org/10.1042/bj2350747.
- 33. Le Guillouzer S, Groleau MC, Mauffrey F, Deziel E. 2020. ScmR, a global regulator of gene expression, quorum sensing, pH homeostasis, and

- virulence in Burkholderia thailandensis. J Bacteriol 202:e00776-19. https://doi.org/10.1128/JB.00776-19.
- Mao D, Bushin LB, Moon K, Wu Y, Seyedsayamdost MR. 2017. Discovery of ScmR as a global regulator of secondary metabolism and virulence in Burkholderia thailandensis E264. Proc Natl Acad Sci U S A 114:E2920–E2928. https://doi.org/10.1073/pnas.1619529114.
- Maddocks SE, Oyston PC. 2008. Structure and function of the LysR-type transcriptional regulator (LTTR) family proteins. Microbiology (Reading) 154:3609–3623. https://doi.org/10.1099/mic.0.2008/022772-0.
- 36. Rho S, Jung W, Park JK, Choi MH, Kim M, Kim J, Byun J, Park T, Lee BI, Wilkinson SP, Park S. 2022. The structure of Deinococcus radiodurans transcriptional regulator HucR retold with the urate bound. Biochem Biophys Res Commun 615:63–69. https://doi.org/10.1016/j.bbrc.2022.05.034.
- Banin E, Vasil ML, Greenberg EP. 2005. Iron and Pseudomonas aeruginosa biofilm formation. Proc Natl Acad Sci U S A 102:11076–11081. https://doi .org/10.1073/pnas.0504266102.
- Oppy CC, Jebeli L, Kuba M, Oates CV, Strugnell R, Edgington-Mitchell LE, Valvano MA, Hartland EL, Newton HJ, Scott NE. 2019. Loss of O-linked protein glycosylation in Burkholderia cenocepacia impairs biofilm formation and siderophore activity and alters transcriptional regulators. mSphere 4: e00660-19. https://doi.org/10.1128/mSphere.00660-19.
- Hamad MA, Austin CR, Stewart AL, Higgins M, Vazquez-Torres A, Voskuil MI. 2011. Adaptation and antibiotic tolerance of anaerobic Burkholderia pseudomallei. Antimicrob Agents Chemother 55:3313–3323. https://doi .org/10.1128/AAC.00953-10.
- Freiberg JA, Le Breton Y, Harro JM, Allison DL, McIver KS, Shirtliff ME. 2020. The arginine deiminase pathway impacts antibiotic tolerance during biofilm-mediated Streptococcus pyogenes infections. mBio 11:e00919-20. https://doi.org/10.1128/mBio.00919-20.
- 41. Harshey RM, Partridge JD. 2015. Shelter in a swarm. J Mol Biol 427: 3683–3694. https://doi.org/10.1016/j.jmb.2015.07.025.
- Jacobs JL, Fasi AC, Ramette A, Smith JJ, Hammerschmidt R, Sundin GW. 2008. Identification and onion pathogenicity of Burkholderia cepacia complex isolates from the onion rhizosphere and onion field soil. Appl Environ Microbiol 74:3121–3129. https://doi.org/10.1128/AEM.01941-07.
- 43. Kearns DB. 2010. A field guide to bacterial swarming motility. Nat Rev Microbiol 8:634–644. https://doi.org/10.1038/nrmicro2405.
- Erhardt M. 2016. Strategies to block bacterial pathogenesis by interference with motility and chemotaxis. Curr Top Microbiol Immunol 398: 185–205. https://doi.org/10.1007/82\_2016\_493.
- Urban TA, Griffith A, Torok AM, Smolkin ME, Burns JL, Goldberg JB. 2004.
  Contribution of Burkholderia cenocepacia flagella to infectivity and inflammation. Infect Immun 72:5126–5134. https://doi.org/10.1128/IAI.72.9.5126-5134.2004.
- 46. Zlosnik JE, Mori PY, To D, Leung J, Hird TJ, Speert DP. 2014. Swimming motility in a longitudinal collection of clinical isolates of Burkholderia cepacia complex bacteria from people with cystic fibrosis. PLoS One 9: e106428. https://doi.org/10.1371/journal.pone.0106428.
- Chua KL, Chan YY, Gan YH. 2003. Flagella are virulence determinants of Burkholderia pseudomallei. Infect Immun 71:1622–1629. https://doi.org/ 10.1128/IAI.71.4.1622-1629.2003.

- Rossi E, Paroni M, Landini P. 2018. Biofilm and motility in response to environmental and host-related signals in Gram negative opportunistic pathogens. J Appl Microbiol 125:1587–1602. https://doi.org/10.1111/jam.14089.
- 49. Williamson KS, Richards LA, Perez-Osorio AC, Pitts B, McInnerney K, Stewart PS, Franklin MJ. 2012. Heterogeneity in Pseudomonas aeruginosa biofilms includes expression of ribosome hibernation factors in the antibiotic-tolerant subpopulation and hypoxia-induced stress response in the metabolically active population. J Bacteriol 194:2062–2073. https://doi.org/10.1128/JB.00022-12.
- Kramer J, Ozkaya O, Kummerli R. 2020. Bacterial siderophores in community and host interactions. Nat Rev Microbiol 18:152–163. https://doi.org/10.1038/s41579-019-0284-4.
- Hillerich B, Westpheling J. 2008. A new TetR family transcriptional regulator required for morphogenesis in Streptomyces coelicolor. J Bacteriol 190: 61–67. https://doi.org/10.1128/JB.01316-07.
- Sivapragasam S, Grove A. 2016. Streptomyces coelicolor XdhR is a direct target of (p)ppGpp that controls expression of genes encoding xanthine dehydrogenase to promote purine salvage. Mol Microbiol 100:701–718. https://doi.org/10.1111/mmi.13342.
- Radi R, Tan S, Prodanov E, Evans RA, Parks DA. 1992. Inhibition of xanthine oxidase by uric acid and its influence on superoxide radical production. Biochim Biophys Acta 1122:178–182. https://doi.org/10.1016/0167-4838(92)90321-4.
- 54. Alexeyev MF. 1999. The pKNOCK series of broad-host-range mobilizable suicide vectors for gene knockout and targeted DNA insertion into the chromosome of gram-negative bacteria. Biotechniques 26: 824–828. https://doi.org/10.2144/99265bm05.
- Winsor GL, Khaira B, Van Rossum T, Lo R, Whiteside MD, Brinkman FS. 2008. The Burkholderia Genome Database: facilitating flexible queries and comparative analyses. Bioinformatics 24:2803–2804. https://doi.org/10 .1093/bioinformatics/btn524.
- 56. Jumper J, Evans R, Pritzel A, Green T, Figurnov M, Ronneberger O, Tunyasuvunakool K, Bates R, Zidek A, Potapenko A, Bridgland A, Meyer C, Kohl SAA, Ballard AJ, Cowie A, Romera-Paredes B, Nikolov S, Jain R, Adler J, Back T, Petersen S, Reiman D, Clancy E, Zielinski M, Steinegger M, Pacholska M, Berghammer T, Bodenstein S, Silver D, Vinyals O, Senior AW, Kavukcuoglu K, Kohli P, Hassabis D. 2021. Highly accurate protein structure prediction with AlphaFold. Nature 596:583–589. https://doi.org/10.1038/s41586-021-03819-2.
- Kim S, Chen J, Cheng T, Gindulyte A, He J, He S, Li Q, Shoemaker BA, Thiessen PA, Yu B, Zaslavsky L, Zhang J, Bolton EE. 2019. PubChem 2019 update: improved access to chemical data. Nucleic Acids Res 47:D1102–D1109. https://doi.org/10.1093/nar/gky1033.
- Liu Y, Grimm M, Dai WT, Hou MC, Xiao ZX, Cao Y. 2020. CB-Dock: a web server for cavity detection-guided protein-ligand blind docking. Acta Pharmacol Sin 41:138–144. https://doi.org/10.1038/s41401-019-0228-6.
- Pettersen EF, Goddard TD, Huang CC, Meng EC, Couch GS, Croll TI, Morris JH, Ferrin TE. 2021. UCSF ChimeraX: structure visualization for researchers, educators, and developers. Protein Sci 30:70–82. https://doi.org/10.1002/ pro.3943.
- Panday A, Xiao L, Grove A. 2015. Yeast high mobility group protein HMO1 stabilizes chromatin and is evicted during repair of DNA double strand breaks. Nucleic Acids Res 43:5759–5770. https://doi.org/10.1093/nar/ gkv498.